Heat Transfer Modeling and Computational Experiment for Uranium Dioxide Fuel Fragment Surrounded by Concrete

JAMSHID GHARAKHANLOU[3], IVAN V. KAZACHKOV[1,2], SERGE V. CHERNYSHENKO[4]

[1]Dept of Energy Technology, Royal Institute of Technology, Stockholm, 10044, УГ GF GP
[2]Dept of Applied Mathematics and Informatics, Nizhyn Gogol State University, WMГ CKP G
[3]Dept of Heat and Power, National Technical University of Ukraine "KPI", UKRAINE
[4]Information Systems Institute, University Koblenz-Landau, GERMANY

Abstract: - The problem is of interest for nuclear power safety and some other fields. Non-stationary two-dimensional boundary task for non-linear heat flow process in cylindrical rod of dioxide uranium surrounded by cylindrical concrete layer is considered with account of the real physical properties of materials depending on temperature, as well as accounting an internal heat generation of radioactive material. The mathematical model of a heat transfer process is realized as computer program for the FLEX PDE platform. Based on the model the computational experiments have been performed and their analysis was made. The results obtained maybe useful by performing the nuclear safety analysis, as well as by model calculations in constructing the passive protection systems against severe accidents at the nuclear power plants.

Keywords: heat transfer process, non-stationary, rod, uranium dioxide, concrete, computational experiment.

1 Problem description and actuality

Non-stationary heat transfer tasks for melt-fuel interaction during severe accidents and other similar problems are of great importance for theory and engineering practices 1-12].

Model physical situations for the fragments of radioactive fuel surrounded by concrete are in focus of the heat transfer processes studied in this paper. Cylindrical configurations of Uranium dioxide in a concrete (UO_2) cover are analyzed in different scenario, various parameters and sizes of the fuel rod and surrounding concrete.

Non-stationary heat transfer processes are considered in a simplified statement about 2-D processes neglecting the changes along the rod. It is assumed that the main changes are in a cross sectional area of the system. And the focus is directed to influence of the real physical properties, which substantially depend on temperature. Such problem is of importance for example in modeling the heat transfer processes during severe accidents at nuclear power plants where high-temperature processes are going fast and a lot of completely different physical situations happen.

2 Basic equations

2.1 The heat flow equations

The heat flow equations for modeling the above-mentioned processes are based on energy conservation law. In dimension form energy conservation equations for Uranium dioxide and concrete are written as follows:

$$\rho_1 c_1 d\left(T_1\right)/dt = div(k_1 \cdot gradT_1) + q_1, \qquad (1)$$

$$\rho_2 c_2 d\left(T_2\right)/dt = div(k_2 \cdot gradT_2), \qquad (2)$$

where T- temperature (by Kelvin), t- time, ρ, c, k – corresponding density, heat capacity and conduction coefficients for Uranium dioxide (1) and concrete (2). q_1 is intensity of internal heat generation (all values are in SI). For fresh fuel $q=10^9$ W/m^3, for spent fuel – about $q=2*10^5$ W/m^3.

The equations (1), (2) can be transformed to dimensionless form:

$$\bar{\rho}_1 \cdot \bar{c}_1 \cdot \frac{\partial \theta_1}{\partial Fo} = div(\bar{k}_1 \cdot grad\theta_1) + Q_1, \qquad (3)$$

$$\bar{\rho}_2 \cdot \bar{c}_2 \cdot \gamma \frac{\partial \theta_2}{\partial Fo} = div(\bar{k}_2 \cdot grad\theta_2), \qquad (4)$$

where the dashed values are dimensionless parameters, with relation to the following their scales, respectively: temperature T_0, length R_1, time R_1^2 / a_{l0}. θ is dimensionless temperature, $Fo = ta_{10}/R_1^2$ - Fourier number, $a = k/(\rho c)$ - heat diffusivity coefficient, R_2, R_1 - the radiuses of concrete and fuel rod, $Q_1 = q_1 R_1^2/(k_{10}T_0)$, $\gamma = a_{10}/a_{20}$. Zero indices point the corresponding values by the stated characteristic temperature.

2.2 Boundary and initial conditions

Initial conditions contain the accepted known distribution of all functions at the initial moment of time. Axial symmetry condition for the system is adopted too, which simplifies the boundary 3-D problem making it 2-D. Also equal temperatures and heat fluxes are supposed for the phases at the interfacial boundaries of their contact. For the external surface of the concrete region it is stated heat transfer condition from concrete to a surrounding medium. Thus it yields:

$$t = 0, \quad T = T_i^0(x, y), \quad i=1,2; \qquad (5)$$

$$x = y = 0, \quad \partial T_1/\partial r = 0; \qquad (6)$$

$$x^2 + y^2 = R_1^2, \quad k_1 \, \partial T_1/\partial r = k_2 \, \partial T_2/\partial r; \qquad (7)$$

$$x^2 + y^2 = R_2^2, \quad k_2 \, \partial T_2/\partial r = -\alpha_2 \left(T_2 - T_c\right). \qquad (8)$$

Here T_c is temperature of surrounding medium outside the region occupied by concrete, α_2 - heat transfer coefficient for concrete, r - direction by the radiuses of cylinders (normal to cylindrical surfaces of the fuel and concrete).

For dimensionless equations (3), (4) the boundary and initial conditions (5)-(8) are transformed to a form

$$t = 0, \quad \theta_i = \theta_i^0(x, y); \qquad (9)$$

$$\bar{x} = \bar{y} = 0, \quad \partial \theta_1/\partial n = 0; \qquad (10)$$

$$\bar{x}^2 + \bar{y}^2 = 1, \quad \beta \, \partial \theta_1/\partial n = \partial \theta_2/\partial n; \qquad (11)$$

$$\bar{x}^2 + \bar{y}^2 = \delta^2, \quad \partial \theta_2/\partial n = -Nu / \left(\bar{k}_2 \cdot \delta\right) \cdot \left(\theta_2 - \theta_s\right). \qquad (12)$$

where n is normal to surface direction, $\beta = k_1 / k_2$, $\bar{k}_2 = k_2 / k_{20}$, $\delta = R_2 / R_1$, $Nu = \alpha_2 R_2 / k_{20}$ - Nusselt number (ratio of external to internal thermal resistance, or heat fluxes due to heat transfer to surrounding compared to conductivity in a concrete layer). Zero indices mean characteristic scales and the parameters by such corresponding scaling values. Thus, the regularities of the physical system are completely determined by Fo, Nu, intensity of internal heat generation Q_1, and simplexes γ, δ, β determining the ratios of heat diffusivities, sizes of the regions (fuel and concrete) and heat conductivity coefficients for fuel and concrete

3 Physical properties and their dependence on temperature

Diverse combinations of the physical properties substantially depending on temperature predetermine a number of quite different regimes and peculiarities for the high-speed and high-temperature heat flow processes.

For example uncertainties in the corium properties and their dynamic high-speed variation cause big problem by studying the severe accidents' scenarios. Uncertainties of the hypothetic scenarios are complicated with uncertainties of the corium parameters starting from its content (!).

Physical properties vary in a wide range: density, viscosity, conductivity, surface tension, heat capacity of the liquid and solid phases, heat of phase transition, etc. One can imagine how much different combinations and physical situations are available due to this. Therefore mathematical modeling and computer simulation in a wide range of varying parameters may help to identify the main classes of the systems and their most crucial regimes.

3.1 Physical properties of nuclear fuel, coolant and concrete and their dependence on temperature

According to [13] the heat conductivity, heat capacity and density of nuclear fuel are non-linear functions of temperature, which are polynomial approximated as follows:

$$k_1 = 10,7 - 9,6 \cdot 10^{-3} T + 3,43 \cdot 10^{-6} T^2 - 3,49 \cdot 10^{-10} T^3; \qquad (13)$$

$$c_1 = 2209,9 + 2,7773 \, T - 0,0027 \, T^2 + 10^{-6} T^3 - 10^{-10} T^4; \qquad (14)$$

$$\rho_1 = 10620 - 51,473 T - 2,4621 T^2; \qquad (15)$$

All approximations are valid in the range of temperatures from about 300 °K to 3000 °K (over melting temperature). More detail data are available from [14-17]. Some of them are given in the Tables 1-3.

3.1.1 Properties of Uranium fuel

Table 1 contains thermodynamic properties of the Uranium dioxide (UO_2) by standard density in solid and liquid states. Table 2 shows comparative physical characteristics of the fuel and some modeling melts used in experimental studies [1-4].

Analysis of the data presented in the Table 1 shows that a lot of different qualitative regimes are available due to changes in properties, which means that by high-speed temperature variation the system behaviors may dramatically change in time.

3.1.2 Properties of mixtures of fuel and other materials

Mixtures of Uranium dioxide UO_2 and different materials: $UO_2 + BeO$, ThO_2, Al, C, Y_2O_3, U_3O_8, etc. versus temperature are presented in the Table 3, where from the properties needed may be chosen.

Table 1. The thermodynamic properties of the Uranium dioxide (UO_2) by standard density in solid (top part) and liquid (bottom part) states

Твердое состояние UO_2

M=270 $T_{пл}$=2850°C =3120 ± 30K $Q_{пл}$=277,1 ± 3,7кДж/кг

t, °C	T, K	ρ, кг/м³	C_p, Дж/кг	λ, Вт/м·К	Λ(T), Вт/м	a, 10⁻⁶ м²/с	β, 10⁻⁵ К⁻¹
0	273	10960	228	10,35	0	4,14	2,926
27	300	10951	236	9,70	301	3,75	2,927
100	373	10928	256	8,46	934	3,03	2,932
200	473	10896	275	7,15	1711	2,38	2,946
300	573	10864	288	6,19	2375	1,98	2,969
400	673	10831	297	5,46	2956	1,70	2,998
500	773	10799	302	4,88	3472	1,50	3,036
600	873	10766	306	4,41	3936	1,34	3,082
650	923	10749	308	4,21	4152	1,27	3,107
700	973	10733	310	4,03	4358	1,21	3,136
800	1073	10699	315	3,71	4744	1,10	3,171
900	1173	10664	319	3,43	5101	1,01	3,256
1000	1273	10628	324	3,20	5432	0,93	3,362
1100	1373	10591	328	3,10	5590	0,89	3,490
1132	1405	10579	329	3,00	5742	0,86	3,562
1200	1473	10552	330	2,84	6034	0,81	3,721
1300	1573	10512	333	2,70	6311	0,77	3,901
1400	1673	10470	336	2,60	6576	0,74	4,102
1500	1773	10426	342	2,52	6832	0,71	4,323
1600	1873	10380	349	2,47	7081	0,68	4,565
1700	1973	10331	361	2,46	7327	0,66	4,828
1800	2073	10280	376	2,47	7573	0,64	5,111
1900	2173	10226	397	2,51	7821	0,62	5,414
2000	2273	10169	424	2,57	8075	0,60	5,737
2100	2373	10109	458	2,66	8336	0,57	6,081
2200	2473	10046	500	2,78	8608	0,55	6,444
2300	2573	9979,3	550	2,92	8893	0,53	6,827
2400	2673	9909,4	619	3,07	9192	0,50	7,230
2500	2773	9835,9	619	3,25	9508	0,53	7,652
2600	2873	9758,8	619	3,44	9842	0,57	8,094
2700	2973	9678,1	619	3,64	10196	0,61	8,555
2800	3073	9593,5	619	3,86	10571	0,65	9,036

Жидкое состояние UO_2

M=270 $T_{кип}$=3640°C =3820K ± 50K $Q_{исп}$=1530кДж/кг

t, °C	T, K	ρ, кг/м³	$C_{вl}$, Дж/кг·К	λ, Вт/(м·К)	μ, мПа/с	a, 10⁻⁷ м²/с	β, 10⁻⁴ К⁻¹	σ, мН/м	P, МПа
2850	3123	8857,2	505	2,5	4,34	6,0	1,048	512	0,00469
2900	3173	8810,8	489	—	4,24	—	1,054	503	0,00625
3000	3273	8717,9	460	—	4,05	—	1,065	484	0,0104
3100	3373	8625,1	433	—	3,89	—	1,077	465	0,0169
3200	3473	8532,2	408	2,8	3,74	8,2	1,088	446	0,0264
3300	3573	8439,4	386	—	3,60	—	1,100	427	0,0403
3400	3673	8346,5	365	—	3,48	—	1,112	408	0,0599
3500	3773	8253,7	346	—	3,36	—	1,125	389	0,0871
3600	3873	8160,8	328	—	3,26	—	1,138	370	0,124
3700	3973	8068,0	312	—	3,16	—	1,151	351	0,173
3800	4073	7975,1	297	—	3,07	—	1,164	332	0,237
3900	4173	7882,3	283	—	2,99	—	1,178	313	0,320
4000	4273	7789,4	270	—	2,91	—	1,192	294	0,424
4100	4373	7696,6	258	—	2,84	—	1,206	—	0,555
4200	4473	7603,7	246	3,6	2,78	11,0	1,221	—	0,716
4300	4573	7510,9	236	—	2,71	—	1,236	—	0,913
4400	4673	7418,0	226	—	2,66	—	1,252	—	1,15
4500	4773	7325,2	216	—	2,60	—	1,268	—	1,43
4600	4873	7232,3	208	—	2,55	—	1,284	—	1,77
4700	4973	7139,5	199	—	2,50	—	1,301	—	2,16
4800	5073	7046,6	192	—	2,46	—	1,318	—	2,61
4900	5173	6953,8	184	—	2,41	—	1,335	—	3,14
5000	5273	6860,9	177	—	2,37	—	1,353	—	3,74
5100	5373	6768,1	171	—	2,33	—	1,372	—	4,42
5200	5473	6675,2	165	—	2,30	—	1,391	—	5,19
5300	5573	6582,4	159	—	2,26	—	1,411	—	6,05
5400	5673	6489,5	153	—	2,23	—	1,431	—	7,01
5500	5773	6396,7	148	—	2,20	—	1,452	—	8,07
5600	5873	6303,8	143	—	2,17	—	1,473	—	9,25

Table 2. Comparative physical characteristics of the fuel and modeling melts used in experiments
и моделирующих расплавов

PROPERTY	Corium (UO_2-ZrO_2) (80-20 Wt%)	CaO-B_2O_3 (30-70 Wt%)	MnO-TiO_2 (78-22 Wt%)	CaO-WO_3 (5-95 Wt%)	Al_2O_3
Melting point (K)	2900	1300	1650	1525	2300
Density (Kg/m³)	8000	2500	4500	6500	2500
Viscosity (Pa.s)	0.005	0.1 – 0.3	------	------	0.004
Thermal Conductivity (W/m.K)	10	3.0	------	------	8
Surface tension (N/m)	1.0	0.15	------	------	0.5
Specific heat (J/Kg.K)	540	2200	900	500	775

As it is seen from the Tables 1, 2, one can choose the non-radioactive materials with right properties for modeling the severe accidents scenarios or some other physical systems [1-5] for investigation the important crucial phenomena.

3.2 Development of the new modeling melts

In some cases researchers need the materials with specific physical properties, which are not available among the known materials. Then such new materials may be developed specially for the goal stated. The new materials have been developed at the Royal Institute of Technology (KTH) for conducting the experimental study of the hypothetical severe accidents' scenarios [4]:

- CaO-B_2O_3, mass fraction (wt/o) 30:70, density ~2500, melting temperature: 1250 °K (solidus), 1300 °K (liquidus), crucible: carbon steel or stainless steel (better), bad SiC;
- TiO_2-MnO_2, mass fraction (wt/o) 18.7:81.3, mol fraction (m/o) 20:80, density ~4500, melting temperature: 1620 °K (liquidus), 1520 °K (solidus): TiO_2 (25kg), MnO_2 (50kg), crucible: carbon steel or stainless steel (better), bad SiC;

Table 3. Physical properties of the mixtures of Uranium dioxide UO_2 with different materials: UO_2+BeO, ThO_2, Al, C, Y_2O_3, U_3O_8, etc.

Состав смеси, вес. %	γ, 10^3 кг/м³	Содержание U в 1 м³ смеси, кг	c_p, кдж/(кг·град)	λ, вт/(м·град)
$100 UO_2$	10,97	9680	0,245	8,7—14,5
$71 UO_2 + 29 BeO$	4,8—4,9	3600	0,432	18,6—20,9
$47 UO_2 + 53 BeO$	3,2—3,6	1900	0,600	23,3—34,9
$10 UO_2 + 90 BeO$	2,3—3,0	300	0,915	83,7—104,7
$10 UO_2 + 90 ThO_2$	10,2	—	0,239	11,2
$60 UO_2 + 40 Al$	4,9	2600	0,472	7,0
$30 UO_2 + 70 Al$	3,5	900	0,711	9,3
$100 BeO$	2,87	—	1,00	160

Теплофизические свойства при 300 °К некоторых спеченных смесей двуокиси урана с графитом

Состав смеси, вес. %	γ, 10^3 кг/м³	Содержание U в 1 м³ смеси, кг	c_p, кдж/(кг·град)	λ, вт/(м·град)	α, 10^{-6} 1/град при 300—1300 °К
100 графита	1,7	—	0,7118	46,0	5,0
$3,8 UO_2 + 96,2 C$	1,75	67	0,6952	20,1	—
$11,7 UO_2 + 88,3 C$	1,88	220	0,6612	18,1	6,3
$19,9 UO_2 + 80,1 C$	1,93	3384	0,6235	17,6	—
$100 UO_2$	10,97	9680	0,2450	11,6	9,2

Теплопроводность двуокиси урана, спеченной с добавками окиси иттрия, вт/(м·град)

T, °К	UO_2	UO_2+4 мол. % Y_2O_3	UO_2+1 мол. % Y_2O_3
373	8,9	—	7,5
473	8,0	—	6,7
573	6,8	6,2	5,9
673	5,8	5,7	5,3
773	5,1	5,5	5,0
873	4,4	5,2	4,7
973	4,0	4,9	4,5
1073	3,6	4,7	4,4
1173	3,5	4,5	4,3
1273	3,4	4,4	4,2
1373	3,3	—	4,3
1473	3,2	—	—
1573	3,2	—	—
1673	3,2	—	—

Коэффициент теплопроводности композиций на основе UO_2, полиэтилена и сажи, вт/(м·град)

T, °К	Полиэтилен	Полиэтилен+ +20 вес. % UO_2	Полиэтилен+ +20 вес. % UO_2+ +20 вес. % сажи
273	0,303	0,313	0,373
283	0,296	0,305	0,356
293	0,290	0,296	0,364
303	0,280	0,285	0,360
313	0,275	0,275	0,353
323	0,270	0,270	0,350
333	0,260	0,260	0,343
343	0,252	0,250	0,335
353	0,246	0,242	0,330
363	0,244	0,240	0,328

- WO_3-CaO eutectics, mass fraction (wt/o) 92.5:7.5, mol fraction (m/o) 75:25, density ~6250, melting temperature: 1470 °K (liquidus), 1410 °K (solidus), crucible: good with SiC.

4 Computational experiment

Modeling and computer simulation have been made in a wide range of the varying parameters to reveal the regularities and important features of the heat flow processes in the system described above.

Dynamics of the system's evolution was determined from solution of the boundary task for equations (3), (4) with the boundary and initial conditions (9)-(12) accounting the non-linear physical properties and approximations (13)-(15).

4.1 The initial data for numerical solution of the boundary task

The initial temperature of the system was taken 20°C (293°K), temperature of the fuel rod 2500°C (2773°K).

The second situation was chosen as initial temperature of the system 20°C but in a center of the fuel rod there is placed point source with a temperature 2500°C. The task is solved with account of the physical properties of the Uranium oxide from temperature.

4.2 Computer program for numerical solution of the boundary task

For numerical solution of the boundary task (3), (4), (9)-(15) the following computer program developed and tested has been used:

```
TITLE  'Transient Conduction in uranium/beton'
SELECT  errlim= 1e-4
VARIABLES  temp
DEFINITIONS
  Lx= 1    r=0.1     R1=0.5    Ly= 1
  k      rcp        { Conductivity and heat capacity }
  tempi= 293          temp0= 2773
  fluxd_x= -k*dx(temp)  heat=10^9
INITIAL VALUES  temp= tempi
EQUATIONS
  rcp* dt(temp)= div(k*grad(temp))+heat
BOUNDARIES
region 1
  k=1.28  rcp=2500*880
  start  (5,-R1)
        arc( center= 0.5*Lx,0.5) angle= 360 close
region 2
  k=-3*10^(-10)*temp^3+3*10^(-6)*temp^2-
0.0096*temp+10.679
```

```
 rcp=10.96*(3*10^(-7)*temp^3-
0.0009*temp^2+1.2464*temp+2592.1)
  start (1,-r)  value(temp)= 2773
          arc( center= 0.5*Lx,0.5) angle= 360 close
{region 3     k= -3*10^(-10)*temp^3+3*10^(-6)*temp^2-
0.0096*temp+10.679
 rcp=0.01096*(3*10^(-7)*temp^3-
0.0009*temp^2+1.2464*temp+2592.1)
 start (0.5,1) point load(temp)=0 line to (0.5*Lx,0.5*Ly)
point value(temp)=temp0}
 TIME
  0 to 36000
PLOTS
  for t= 60, 300, 1200, 3600, 36000
    elevation( temp) from (0.5,Ly/2) to (5,Ly/2)
    elevation( fluxd_x) from (0.5,Ly/2) to (5,Ly/2)
surface(temp)
HISTORIES
   history( temp) at (0.1*Lx,Ly/2) at (0.2*Lx,Ly/2) at
(0.3*Lx,Ly/2)
    at (0.4*Lx,Ly/2) at (0.5*Lx,Ly/2) at (0.6*Lx,Ly/2) at
(0.7*Lx,Ly/2) at (0.8*Lx,Ly/2)
END
```

The computatio was performed in the FLEX PDE platform.

4.3 The results of computations

The situations considered were chosen as follows. Radioactive cylindrical fuel rod surrounded by concrete is prone to heat transfer from the external surface of the concrete (air or water). By different sizes the situation may vary a lot, e.g. fuel rod of 1 cm radius or massive fuel rod 10 sm radius and higher, inside the thin concrete shell or thick concrete layer, etc.

Also the other physical situations were considered, for example, cooling of the hot fuel massive with weak internal heat generation (corium with low concentration of the spent fuel or similar) surrounded by thin or thick concrete layer. The computer simulations allowed revealing some very interesting features of the processes, which may be useful for diverse engineering applications including nuclear power safety problems.

4.3.1 Corium inside the thick concrete layer
by weak internal heat generation

This model task was considered for the initial temperature of concrete 293 °K and corium 2773 °K. Heat conductivity of the concrete was taken equal to 1,28 W/(m·°K), density and specific heat capacity coefficient, respectively, 2500 kg/m^3 and 880 J/(kg·°K). It is supposed that weak effect of internal heat generation supplies constant temperature on the external surface of corium rod, which has initial temperature the same as temperature of the

surrounding concrete massive. Such simplification of the problem statement allows comparably easy modeling of the conjugated boundary task. It allows estimating the intensity of a heat spreading from the narrow surface region of the cylindrical fuel rod into surrounding medium. Some results of computations are presented in Figs 1-4.

The numerical computational grid is presented in Fig. 1. It consists of two circles in the cross section of the physical system of interest: internal fuel rod and external concrete layer.
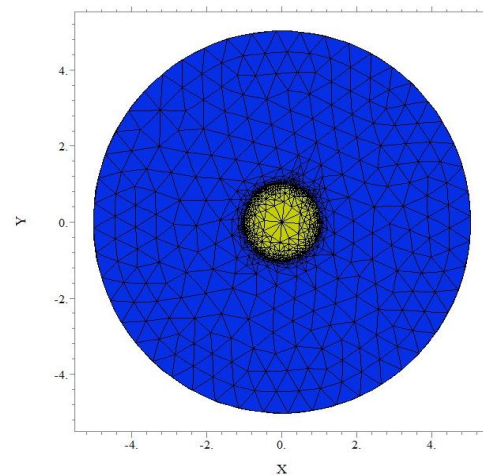
Fig. 1 The numerical computational grid for the conjugated domain of fuel rod and surrounding concrete layer
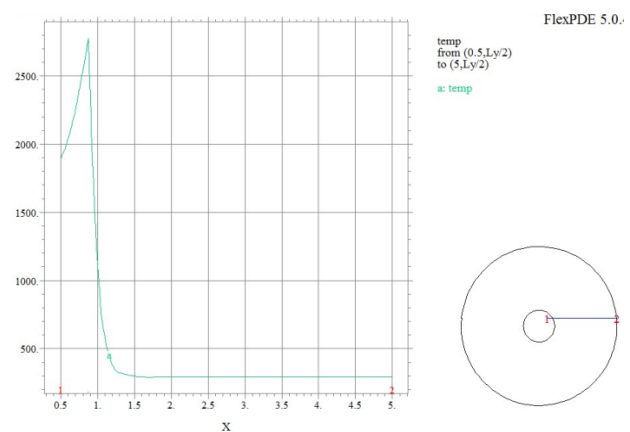

Fig. 2 Distribution of temperature by cross section of fuel and concrete for $t = 1\,\text{h}$

The grid contains huge number of elements built by the method of triangulation. It is adaptively rebuilt at each time step according to the local gradients of parameters. Therefore the most condensed it is in the sub domains with the highest gradients of functions, e.g. on the interface between fuel and concrete where the temperature gradients are the highest. In the rest of the numerical domain the grid nodes are not so small.
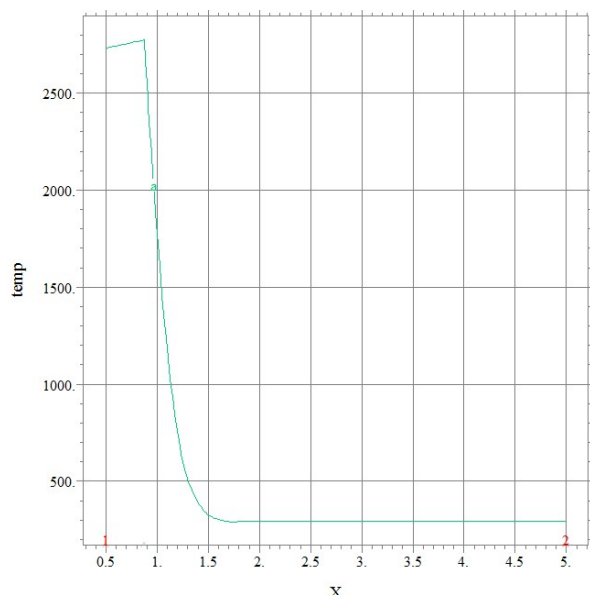
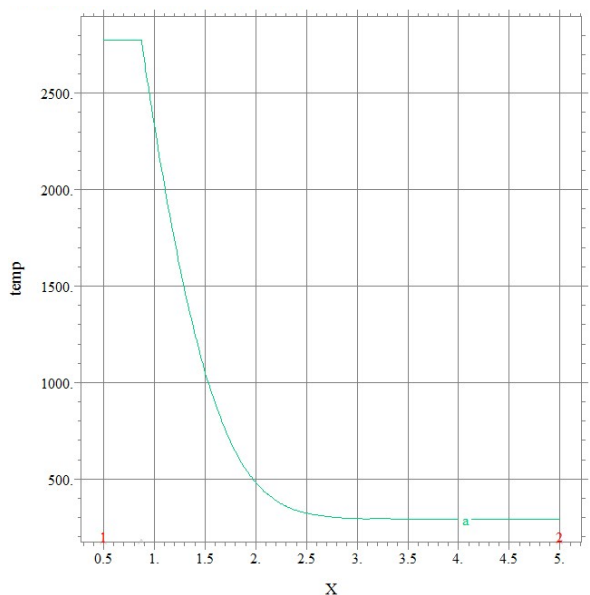Fig. 3 Temperature distribution by cross section of fuel and concrete for   h

Fig. 4 Temperature distribution by cross section of fuel and concrete for $t = 100\,\text{h}$

This computation was made for the fuel radius 1 m and concrete layer radius 5 m. Figs 2-4 show the results for the time from 1 to 100 hours, respectively. Similar picture is observed for the radiuses 0.1 and 0.5 m by time $t = 0.01\,\text{h}$ (0.6 minutes) and for thin rod 0.01 m surrounded by concrete layer of 0.05 m thickness the same picture is observed by $t = 0.0001\,\text{h}$. For this time interval the fuel temperature becomes nearly uniform in the whole region while the concrete still remains cold.

Thus, large scale system is reaching the stationary regime in one day. By this process concrete just starts to warm up getting the temperature 500 °K on a distance about 2 m from the

center. For the medium and large scale systems the same status is reached in one hour and 0.01 h, respectively. And only in 1000 hours the temperature front gets 400 °K by external concrete surface, so that the concrete under such situation firmly serves as heat insulation for fuel rod.

This situation has local character and may be applied for disposal of nuclear waste with low activity.

The large scale system reaches the temperature 2000 °K on the external surface of concrete for ten thousand hours, which is the critical state. The corresponding times for medium and large scale systems are 100 and 1 h.

4.3.2 The case of the same thickness of corium and concrete layers
If the concrete layer's thickness equal to the radius of fuel cylinder, the temperature inside the fuel massive becomes uniform approximately in 100 h, and then the temperature of a concrete is going fast linearly up 800 °K on its external surface.

4.3.3 High temperature in a form of Delta-function in a center of fuel rod
For this case the corresponding computer program is given below, where the domain of the fuel rod is divided into two sub domains, one of which is just point with a high temperature:

```
TITLE    'Transient Conduction in uranium/beton'
SELECT   errlim= 1e-4
VARIABLES  temp
DEFINITIONS
  Lx= 1    r=0.1      R1=0.5     Ly= 1
  k        rcp      { Conductivity and heat capacity }
  tempi= 20   temp0= 2500   fluxd_x= -k*dx(temp)
INITIAL VALUES   temp= tempi
EQUATIONS
  div[-k*grad(temp)]+ rcp* dt(temp)= 0
BOUNDARIES
region 1
 k=128   rcp=2000*840
  start (5,-R1)
       arc( center= 0.5*Lx,0.5) angle= 360 close
region 2
 k=-3*10^(-10)*temp^3+3*10^(-6)*temp^2-
0.0096*temp+10.679
 rcp=10.96*(3*10^(-7)*temp^3-
0.0009*temp^2+1.2464*temp+2592.1)
  start (1,-r)
       arc( center= 0.5*Lx,0.5) angle= 360 close
region 3     k= -3*10^(-10)*temp^3+3*10^(-6)*temp^2-
0.0096*temp+10.679       rcp=0.96*(3*10^(-7)*temp^3-
0.0009*temp^2+1.2464*temp+2592.1)
 start (0.5,1) point load(temp)=0 line to (0.5*Lx,0.5*Ly)
point value(temp)=temp0
 TIME  0 to 36000
```

PLOTS
  for t= 60, 300, 1200, 3600, 36000
    elevation(temp) from (0.5,Ly/2) to (5,Ly/2)
    elevation(fluxd_x) from (0.5,Ly/2) to (5,Ly/2)
    contour(temp)   surface(temp)
HISTORIES
  history(temp) at (0.1*Lx,Ly/2) at (0.2*Lx,Ly/2) at (0.3*Lx,Ly/2)
    at (0.4*Lx,Ly/2) at (0.5*Lx,Ly/2) at (0.6*Lx,Ly/2) at (0.7*Lx,Ly/2) at (0.8*Lx,Ly/2)
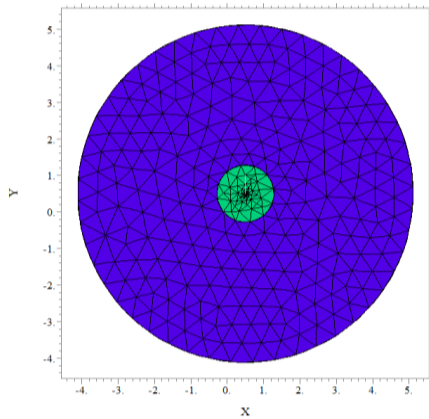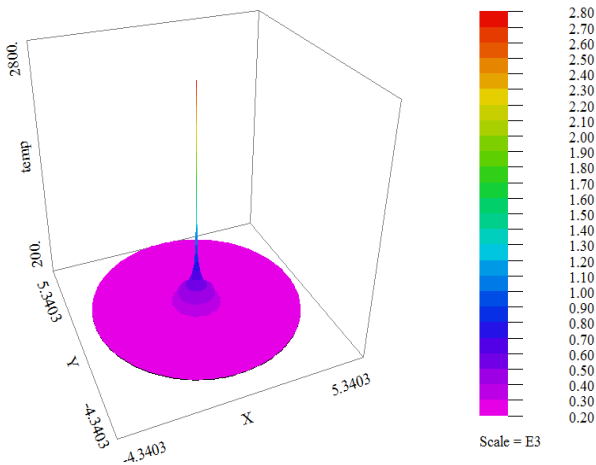END

Fig. 5 Numerical grid of the system

Fig. 6 Temperature distribution from the Delta-
function heat source by   h

The results of computations are presented in Figs 5-7. Fig. 6 shows that for the large scale system $t=10$ temperature distribution in a form of Delta-function still remains in the center of fuel massive even after 10 hours. Fig. 5 evidences that in this case the temperature is smooth by its decrease in all region. Therefore numerical grid is more regular too, without peculiar regions of sharp gradients and grid condensing.

The Fig. 7 shows that even in a layer of fuel massive the temperature is changing comparably slowly, while in the main part of the region occupied by concrete the temperature is practically stable.
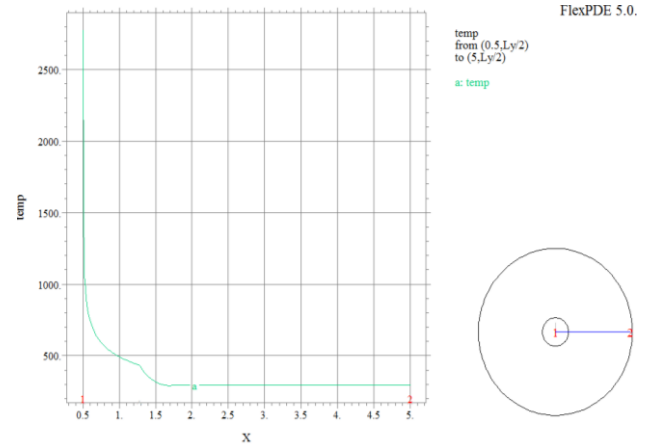
Fig. 7 Temperature by distance from center,   h
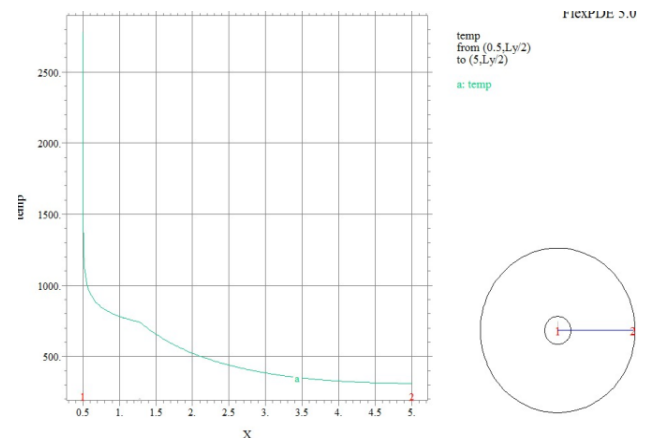
Fig. 8 Temperature from center, $t = 1000$ h

Comparison with the similar data of calculations for the time moments thousand hours presented in Figs 8–10 shows weak changes. Therefore it must be concluded that in this situation an influence of the intensive Delta-function heat source reveals very little and slow.
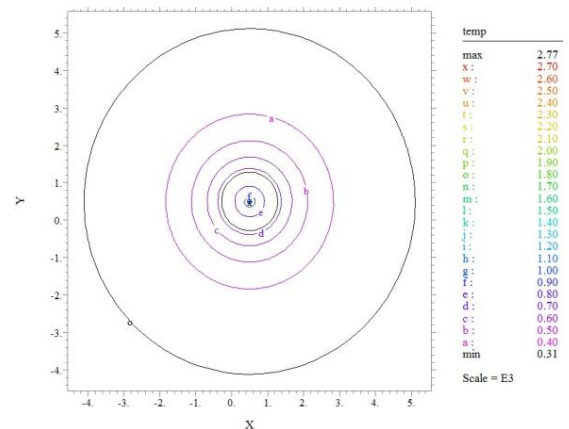
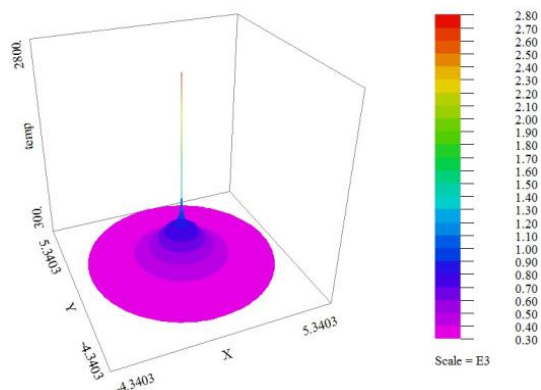Fig. 9 Temperature distribution by distance from center at $t = 1000$ h in a cross section

Fig. 10 Temperature distribution from the Delta-
function heat source by $t = 1000$ h

4.3.4 Fuel massive with internal heat generation surrounded by concrete

The corresponding computer program in the platform FLEX PDE is given below:

```
TITLE   'Transient Conduction in uranium/beton'
SELECT   errlim= 1e-4
VARIABLES   temp
DEFINITIONS
Lx= 1  r=0.1 R1=0.5 Ly= 1  k  rcp {Conductivity and heat
capacity}  heat= 0  tempi=293 temp0= 2773   fluxd_x= -
k*dx(temp)  fluxd_y= -k*dy(temp)
 INITIAL VALUES   temp= 1500
EQUATIONS
    rcp*dt(temp)+ dx( fluxd_x)+dy(fluxd_y)=heat
BOUNDARIES
   region 2
      heat=0  k=1.28   rcp=2500*880
   start (5,0) natural(temp)=(10/1.28)*(temp-tempi)
   arc( center= 0,0) angle= 360 close
   region 1
     heat=10^4           k=-3*10^(-10)*temp^3+3*10^(-
6)*temp^2-0.0096*temp+10.679
     rcp=10.96*(3*10^(-7)*temp^3-
0.0009*temp^2+1.2464*temp+2592.1)
      start  (1,0)   arc( center= 0,0) angle= 360 close
   region 3
   k=-3*10^(-10)*temp^3+3*10^(-6)*temp^2-
0.0096*temp+10.679   rcp=0.01096*(3*10^(-7)*temp^3-
0.0009*temp^2+1.2464*temp+2592.1)
     start (0,0) point natural (temp)=0
   TIME   0 to 3600
   PLOTS   for t= 60, 300, 1200, 3600
   elevation( temp) from (0.5,Ly/2) to (5,Ly/2)
   elevation( fluxd_x) from (0.5,Ly/2) to (5,Ly/2)
surface(temp)
   HISTORIES
 history( temp) at (0.1*Lx,Ly/2) at (0.2*Lx,Ly/2) at
(0.3*Lx,Ly/2)  at (0.4*Lx,Ly/2) at (0.5*Lx,Ly/2) at
(0.6*Lx,Ly/2) at (0.7*Lx,Ly/2) at (0.8*Lx,Ly/2)
   END
```

The calculations were performed by $q=10^4$ (fuel massive has total radioactivity like a spent fuel, e.g.

corium with a lot of mixture) for two cases of the initial temperature in the region (293 and 1500 °K), for the systems of large, medium and small scales. Numerical domain is shown in Fig. 11:
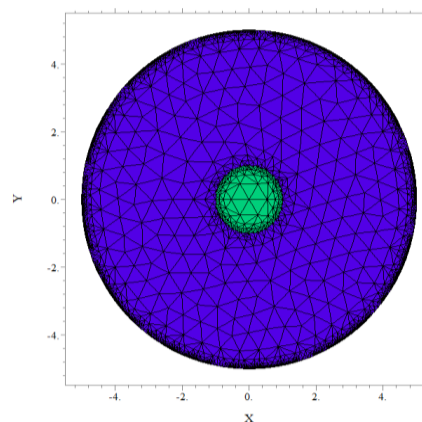

Fig. 11 Numerical domain

where from follows that maximal condensing the triangle grid nodes corresponds to the boundaries of the domain with the maximal temperature gradients.

Some of the results obtained are presented below. Thus, the results for initial temperature 293 °K are shown in Figs. 12-14:
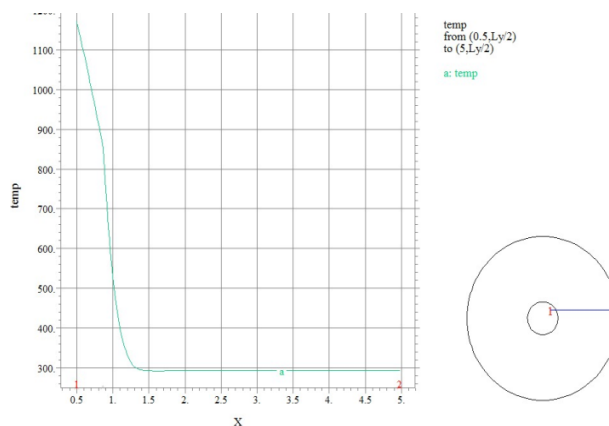

Fig. 12 Temperature field by cross section of the fuel massive and surrounding concrete at   h

As seen from the Fig. 12, the temperature in a center of fuel massive is growing from 293 до 1200 °K in 10 hours in a large scale system (correspondingly in 0.1 h in a system of medium scale and in 0.001 h – in a small scale system), on the boundary interface with concrete – up to 500 °K, and a concrete is heated from 293 to 500 °K only at a distance less than 10% from boundary with fuel massive.

In hundred hours fuel in the center is heated up and melted, at the boundary has the temperature на границе имеет температуру 1500 °K. Concrete

keeps the initial low temperature on a distance from 2.5 to 5 m (in a system of medium scale – from 0.25 to 0.5 m). The dynamics of the temperature field in time in different cross sections of the fuel region is shown in Fig. 14:
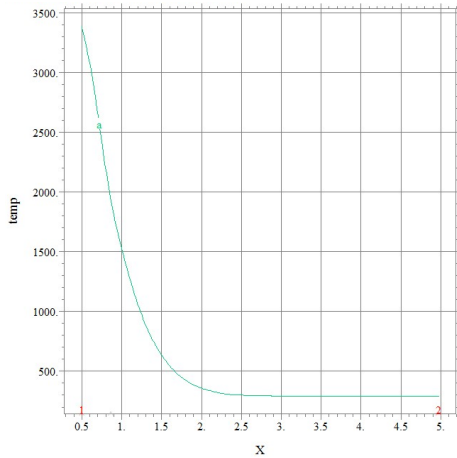

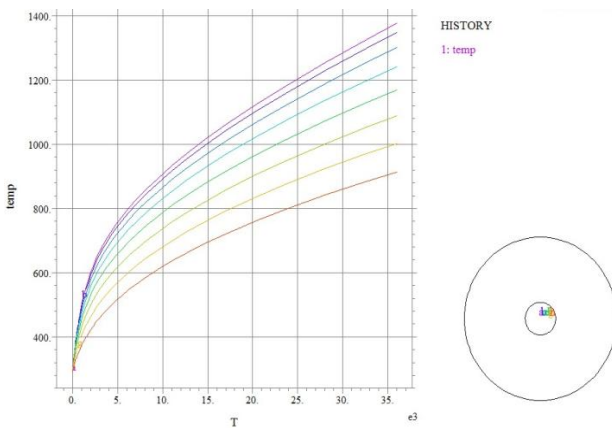Fig. 13 Temperature field by cross section of the fuel massive and surrounding concrete at $t = 100\,\text{h}$

Fig. 14 Evolution of the temperature field by cross section of a fuel in time from 0 to   h

Similar results for initial temperature 1500 °K are given in Figs 15-19. From Figs 15, 16 follows that in 10 h the temperature in a center of fuel massive overwhelms the melting point, while on the boundary it is just 1700 °K. Concrete is heated up to 1700 °K in a thin boundary layer, with nearly the initial temperature 1500 °K in the rest of region. Only on the external boundary of the layer concrete is cooled down from 1500 to 800 °K (temperature of surrounding medium) on a distance of 0.5 m (10% of thickness of the layer).

The clear understanding of the processes give spatial temperature distributions for fuel massive and concrete done in Figs 17, 18. Difference in temperature behaviors of the fuel with time from the center to the boundary presents Fig. 19.
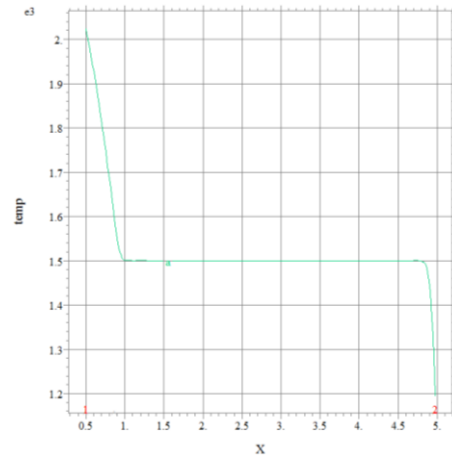

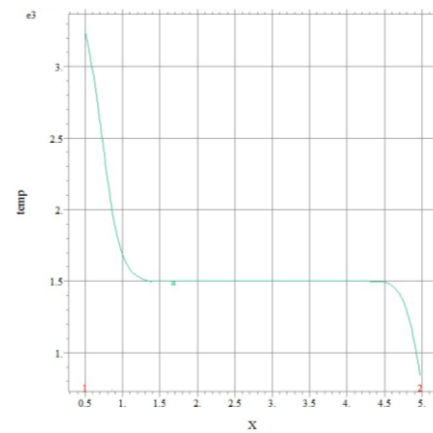Fig. 15 Temperature field by cross section of the fuel massive and surrounding concrete at $t = 1\,\text{h}$

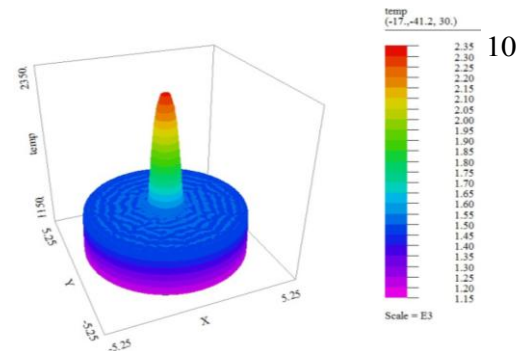Fig. 16 Temperature field by cross section of the fuel massive and surrounding concrete at   h

Fig. 17 Temperature field by cross section of the fuel massive and surrounding concrete at $t = 1\,\text{h}$

5 Conclusions

An analysis of the non-stationary non-linear heat transfer processes for the different scales and physical situation of the fuel rod surrounded by concrete has been done with account of real physical properties dependent on temperature. Influence of all mentioned factors was investigated and regularities of the system revealed. The results obtained are

useful both for the theory and engineering applications, e.g. in analysis of the hypothetic severe accident scenarios at the nuclear power plants and in other important applications.
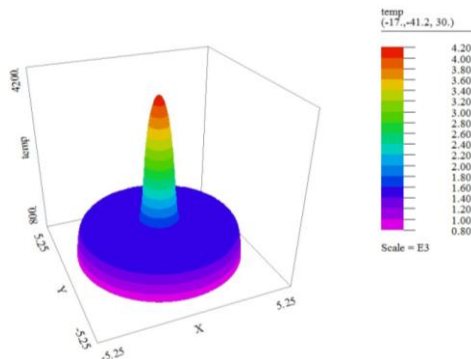

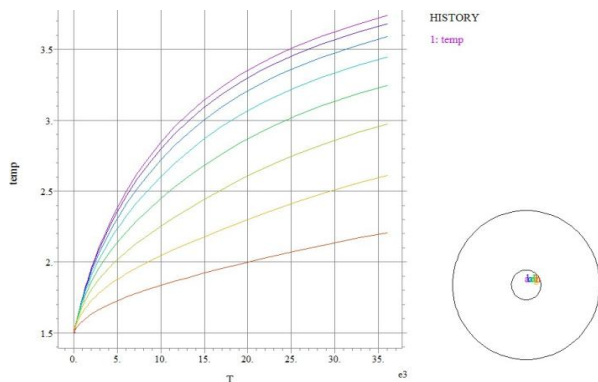Fig. 18 Temperature by cross section of the fuel massive and surrounding concrete at $t = 10$ h

Fig. 19 Temperature evolution by cross section of the fuel massive at $t = 10$ h

References:

[1] Kazachkov I.V. Konovalikhin M.J., Sehgal B.R. Coolability of melt pools and debris beds with bottom injection/ 2nd Jap.-Europ. Two-Phase Flow Group Meeting (Tsukuba, Japan, 2000).- P. 90-96.

[2] Haraldsson H.O., Kazachkov I.V., Dinh T.N., Sehgal B.R. Analysis of thin jet breakup length in immiscible fluids/ Abstr. 3rd Int. Conf. Adv. in Fluid Mechanics (Montreal, Canada, 24-26 May, 2000).- P. 43-47.

[3] Park H.S., Kazachkov I.V., Sehgal B.R. et al. Analysis of Plunging Jet Penetration into Liquid Pool in Isothermal Conditions/ ICMF 2001: 4th Int. Conf. Multiphase Flow (New Orleans, Louisiana, USA, May 27-June 1, 2001).- P.65-69.

[4] Kazachkov I.V., Paladino D., Sehgal B.R. Ex-vessel coolability of a molten pool by coolant injection from submerged nozzles/ 9th Int. Conf. Nucl. Energy Devel (April 8-12, 2001. Nice, France). - P. 43 - 49.

[5] Kazachkov I.V., Konovalikhin M.J., Sehgal B.R. Dryout Location in a Low-porosity Volumetrically Heated Particle Bed// J. of Enhanced Heat Transfer.- 2001.- V.8, No. 6. - P. 397 - 410.

[6] Kazachkov I.V., Konovalikhin M.J. A Model of a Steam Flow through the Volumetrically Heated Particle Bed// Int. J. of Thermal Sciences. - 2002. - Vol. 41. - P. 1077 - 1087.

[7] Kazachkov I.V., Mogaddam Ali Hassan. *Modeling of thermal hydraulic processes during severe accidents at NPP*.- K.: NTUU «KPI», 2008.- 172 c. (In Russian).

[8] Kalvand Ali, Kazachkov I.V. Modeling of Corium Melt Cooling During Severe Accidents at Nuclear Power Plants/ *Recent Advances in Continuum Mechanics (special issue)*/ Proc. IASME/WSEAS Int. Conf.- Univ. of Cambridge, 2009. - P. 200 - 207.

[9] Vakhid Hasani Mogaddam, I.V. Kazachkov. Modeling of corium jet penetration into the pool of volatile coolant under reactor vessel// *Nuclear physics and energy*.- 2010.- №2.- P. 151-158.

[10] Vahid Hasani Moghaddam, I.V. Kazachkov. About modeling of the corium jet penetrating the pool of volatile coolant under reactor vessel/ Int. Conf. on Applied Computer Science (ACS). - Malta, 15-17 September 2010. - p. 89-95.

[11] Kazachkov I.V., Konoval O.V. Non-linear mathematical models for the jets penetrating liquid pool of different density under diverse physical conditions and their simulation// WSEAS transactions on applied and theoretical mechanics. – № 2, Vol. 8, 2013.– P. 156-169.

[12] Konoval O.V., Kalvand Ali, Kazachkov I.V. Modeling of corium cooling and analysis of the factors of containment loading during severe accidents // *Nuclear physics and energy*.- 2013.- P. 276-287. (In Russian).

[13] Rovno NPP. Power Unit № 1. Technical substatiation of the safety of construction and operation of NPP. Attachment 2.- 1998.

Jamshid Gharakhanlou,
Ivan V. Kazachkov, Serge V. Chernyshenko

[14] Chirkin V.S. Thermal physics properties of materials for nuclear installations. M.: Atomizdat.- 1967.- 474 pp. (In Russian).

[15] Kirillov P.L., Bogoslovskaya G.P. Heat transfer in nuclear power installations: Textbook for universities.- M.: Energoatomizdat.- 2000.- 456 pp. (In Russian).

[16] Project for advanced safety analysis of Unit №1 Khmelnitsky AES. Data base by nuclear vapor generating device. BOA 301913-A-R4. 2001.

[17] Krasnoshchekov E.A., Sukomel A.S. Exercises by heat transfer: Textbook. Ed. 4th, redone.- M.: Energiya.- 1980.- 288 pp. (In Russian).